ELEKTROMETALÜRJİ

ELEKTROLİTTE AKIM DAĞILIMI

GENEL BİLGİLER

Elektrometalürjide elektrod yüzeylerinin yapısının önemli etkilerinin olduğu bilinen bir temel bilgidir. Bu bilginin ışığı altında; aım dağılımı;

1. Geometrik şekle,
2. Çözelti ve elektrolitin iletkenliğine,
3. Aşırı gerilimde aktiviteye,
4. Aşırı gerilimde difüzyona,
5. Sistemin hidrodinamiğine bağlıdır.

Akım dağılımının şekli önemlidir. Bunun tespiti WAGNER, NEWMAN bağıntısı ile hesaplanabilir.

Birimsiz WAGNER sayısı;

$$W_a = \frac{d\eta_c}{dj}\frac{\kappa}{l}$$

where $d\eta_c/dj$ is the slope of the cathodic activation overpotential-current density dependence, κ is the conductivity of solution and l is a characteristic length.

Before W_a, the parameter

$$k_c = \kappa \frac{d\eta_c}{dj}$$

was used, according to Kasper[6], Hoar and Agar[7].

Boy kısa, iletkenlik yüksek ve U-I eğrisinin eğimi büyük olmalıdır.

Hücrenin Direnci

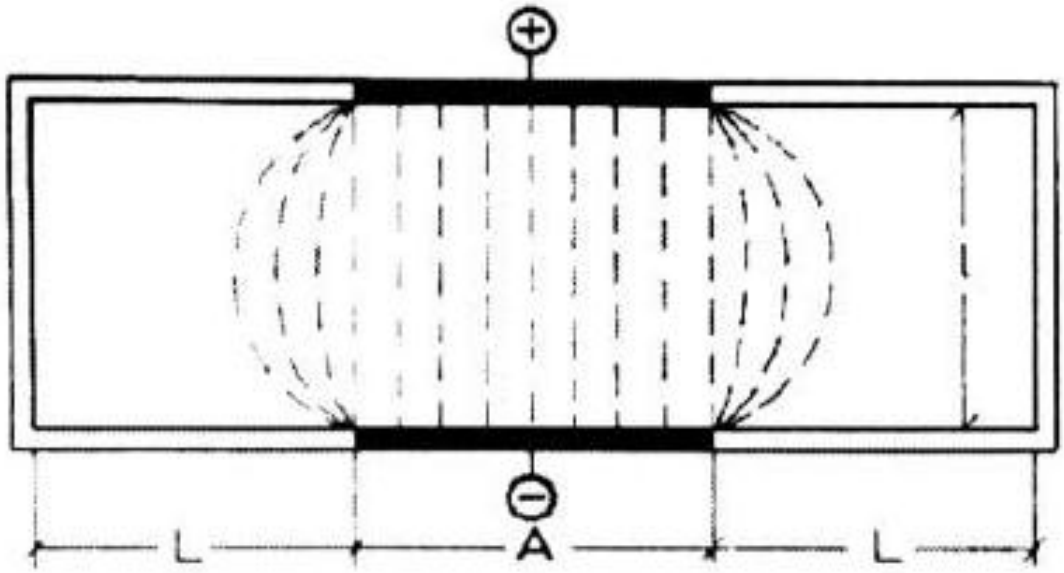

Figure 4.1. Current distribution in a parallel plate electrode geometry (*A* is the electrode width, *L* is the distance between the edge of the electrode and the side walls and *l* is the distance between the electrodes.[9] (Reprinted with permission from the Serbian Chemical Society, Belgrade, Yugoslavia)

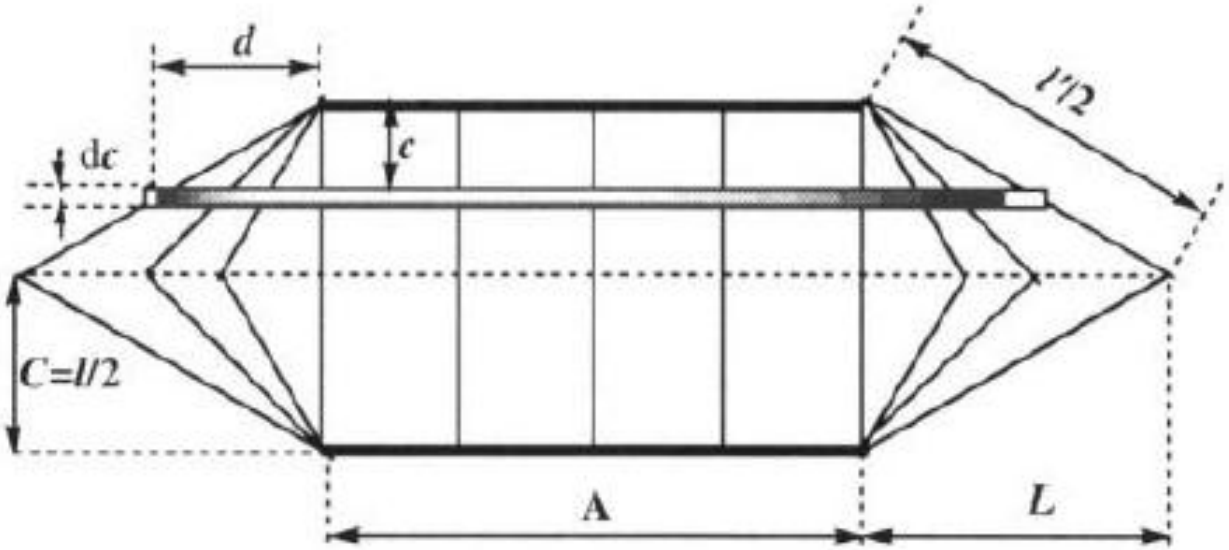

Figure 4.2. The linear approximation model showing the current flow passing around the space between the plane parallel electrodes.[10] (Reprinted with permission from Elsevier Science).

The resistance dR of a section of the electrolyte of thickness dc is given by:

$$dR = \frac{\rho}{B}\frac{dc}{A+2d} \tag{4.1}$$

where B is the height of the electrode and ρ is the specific resistance of the electrolyte. From the linear approximation:

$$d = \frac{L}{C}c \tag{4.2}$$

is obtained. The parameters d and c are indicated in Fig. 4.2.

The resistance of the whole electrolyte is then given by[10]:

$$R = \frac{\rho C}{BL}\ln\left(\frac{A+2L}{A}\right) \tag{4.3}$$

and for $L \rightarrow 0$, by:

$$\lim_{L \to 0} R = \frac{2\rho C}{BA} = \frac{\rho l}{BA} = R_h \qquad (4.4)$$

where R_h corresponds to the resistance of a system with a homogeneous current density distribution (the side walls touch the edges of the electrodes). For $0 \leq L << \infty$, L can be related to A by a linear coefficient k as follows:

$$L = k A \qquad (4.5)$$

which transforms Eq. 4.3 to:

$$R = \frac{R_h}{2k} \ln (1 + 2k) \qquad (4.6)$$

and

$$l_{eff} = \frac{l}{2k} \ln(1 + 2k) \qquad (4.7)$$

taking into account Eq. 4.4, where l_{eff} represents the interelectrode distance in a cell with L=0, the resistance of which is equal to the resistance of a cell in which the interelectrode distance is l and $L > 0$

The cell for the determination of the equivalent resistance is shown in Fig. 4.3.

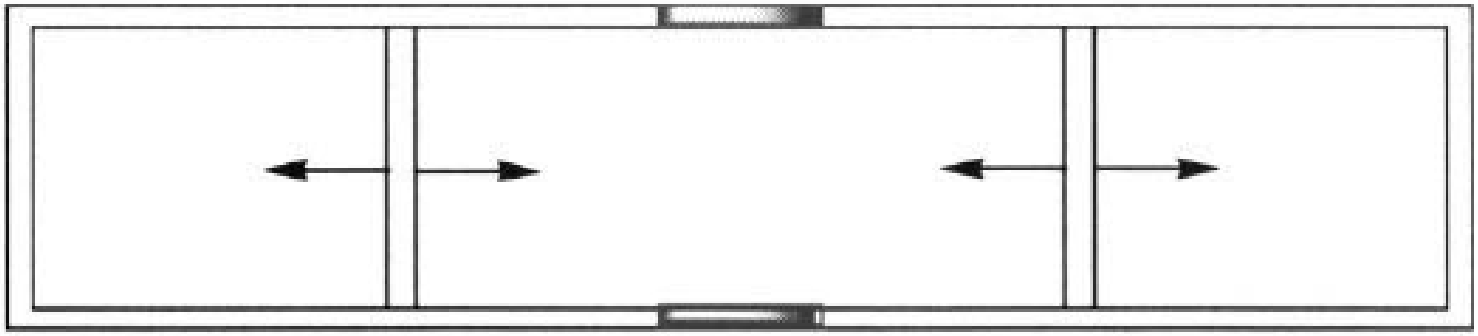

Figure 4.3. Schematic representation of the cell used for the determination of the equivalent resistance.[10] (Reprinted with permission from Elsevier Science).

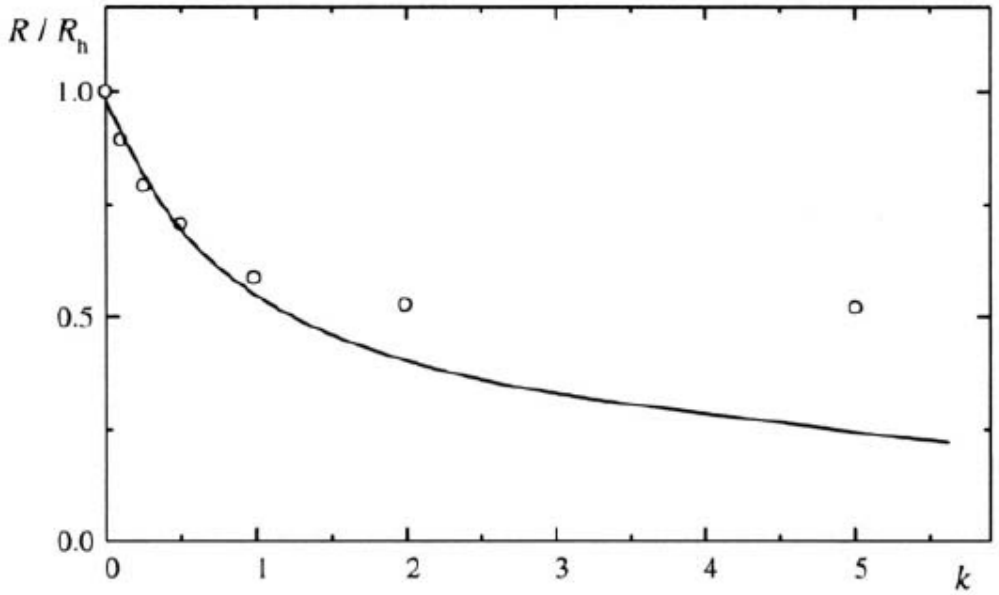

Figure 4.4. The dependence of the total resistance of the system on k: (o) experimentally determined values; (—) calculated values.[10] (Reprinted with permission from Elsevier Science).

Kenar Direnç Etkisi

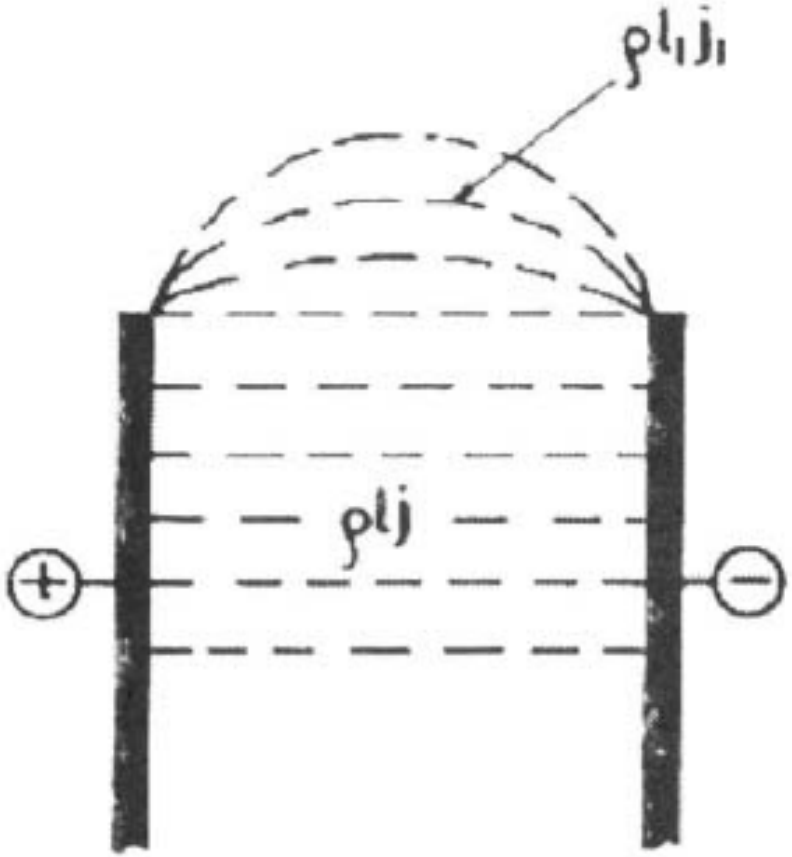

Figure 4.5. Current lines between the electrodes with edges not touching the side walls of the cell.[11] (Reprinted with permission from the Serbian Chemical Society, Belgrade, Yugoslavia).

Hücre gerilimi “U”, denge gerilimi farkı “E”, öz direnç “ρ”, elektrodlar arası “l”, akım yoğunluğu “j”, akım çizgileri arasındaki uzaklık “l_i” ve akım çizgisi nin akım yoğunluğu “j_i” olarak;

$$U - E = \rho\, l\, j$$

Ve

$$U - E = \rho\, l_i\, j_i$$

Olup, $j_i + \Delta j_i - j = U - E \,/\rho(1/l_i - 1/l_i + \Delta l_i)$

ve $j_{c,max} \approx 1{,}3\, j$

Elektrodlar arasındaki minimum uzaklık;

$$l_{eff,e,min} = 2 / (4 - \sqrt{2})\, l$$

$$\rho\, l_i = \rho\, l_{eff,e,min} j_{c,max}$$

Elektrodlar hücre yüzeyine temas etmemelidir.

Elektrodlar arasındaki gerilim;

Homojen olarak, $U = E + \eta_a + \eta_c + \rho l_j$

$$U = E + \eta_{a,e} + \eta_{c,e} + \rho l_{eff,e}\, j_e$$

η_a ve η_c anodik ve katodik akım potansiyeli,

$\eta_{a,e}$ ve $\eta_{c,e}$ anodik ve katodik kenar akım potansiyeli,

$$\eta_{a,e} + \eta_{c,e} = \eta_a + \eta_c - \rho l_{eff,e}\, j_e$$

ve

$$\underline{\rho l_j} = \underline{\rho l_{eff,e}}\, \underline{j_e}$$

The dependences of the current density on the cell voltage for different interelectrode distances and different distances between the edge of the electrode and side wall, for the system **(-)Cu | $CuSO_4$, H_2SO_4, H_2O | Cu(+)** at a temperature of 20° C are shown in Figs. 4.7 – 4.10.

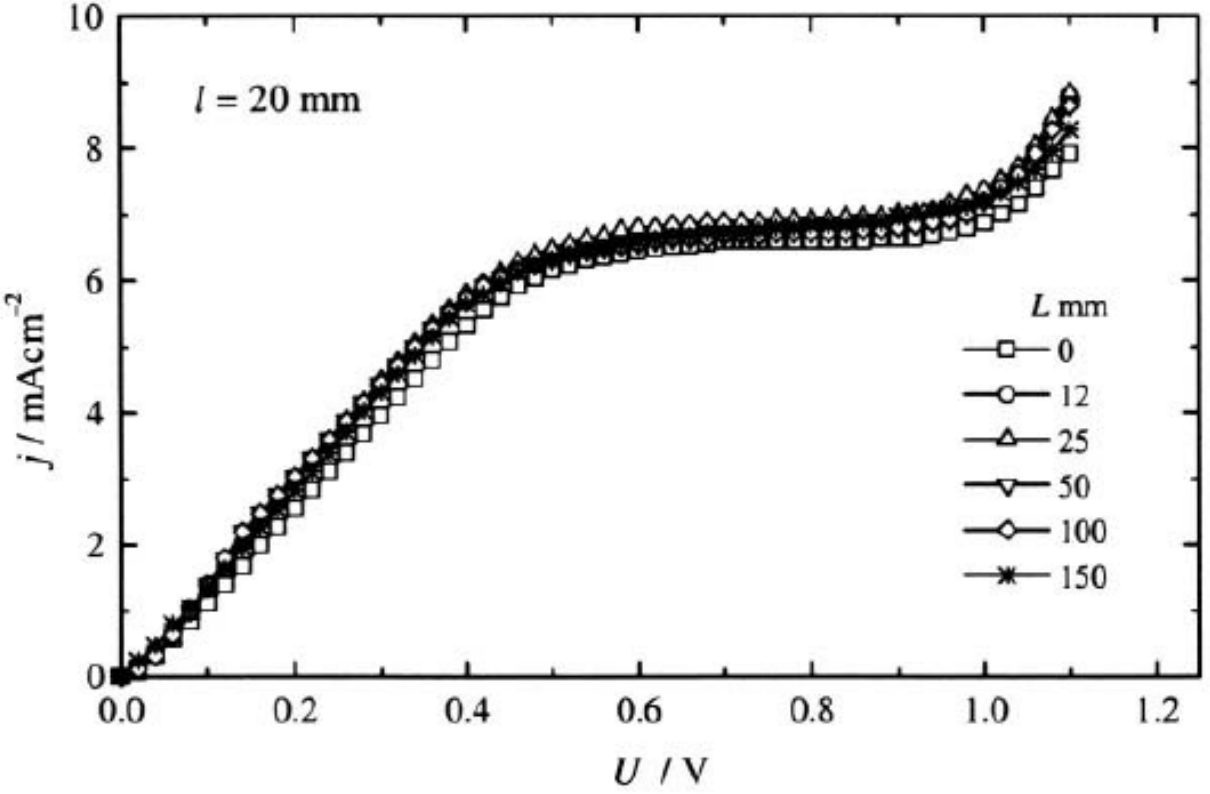

Figure 4.7. **Current density-cell voltage dependencies of the system (-) Cu | 0.1 mol dm^{-3} $CuSO_4$, 0.1 mol dm^{-3} H_2SO_4 | Cu (+) with an interelectrode distance of 20 mm for different distances between the edge of the electrode and the side wall of the cell indicated in the diagram.[9] (Reprinted with permission from the Serbian Chemical Society, Belgrade, Yugoslavia).**

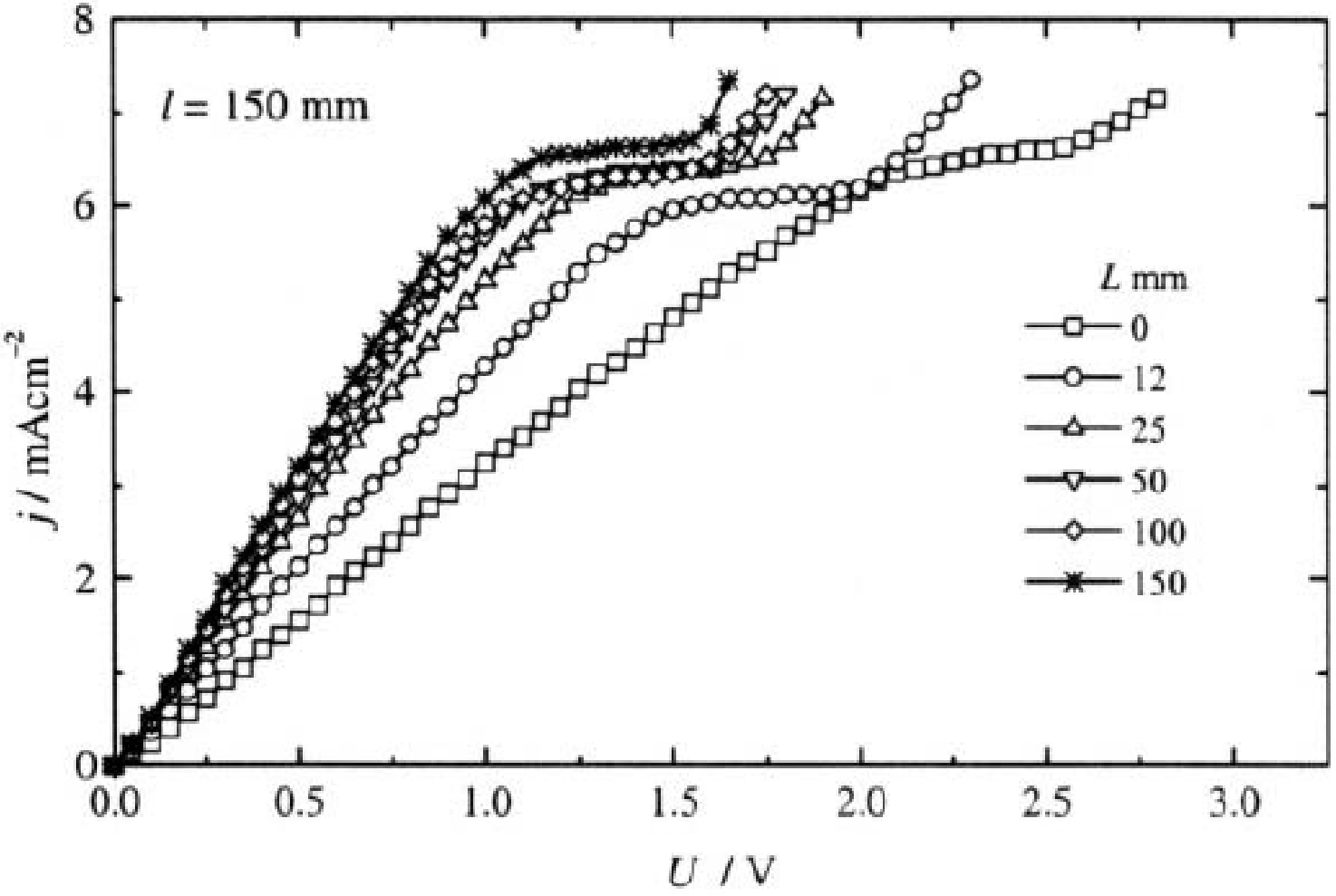

Figure 4.10. Current density-cell voltage dependencies of the system (-) Cu | 0.1 mol dm^{-3} $CuSO_4$, 0.1 mol dm^{-3} H_2SO_4 | Cu with an interelectrode distance of 150 mm for different distances between the edge of the electrode and the side wall of the cell indicated in the diagram.[9] (Reprinted with permission from the Serbian Chemical Society, Belgrade, Yugoslavia).

Akım Yoğunluğunun Değişimi

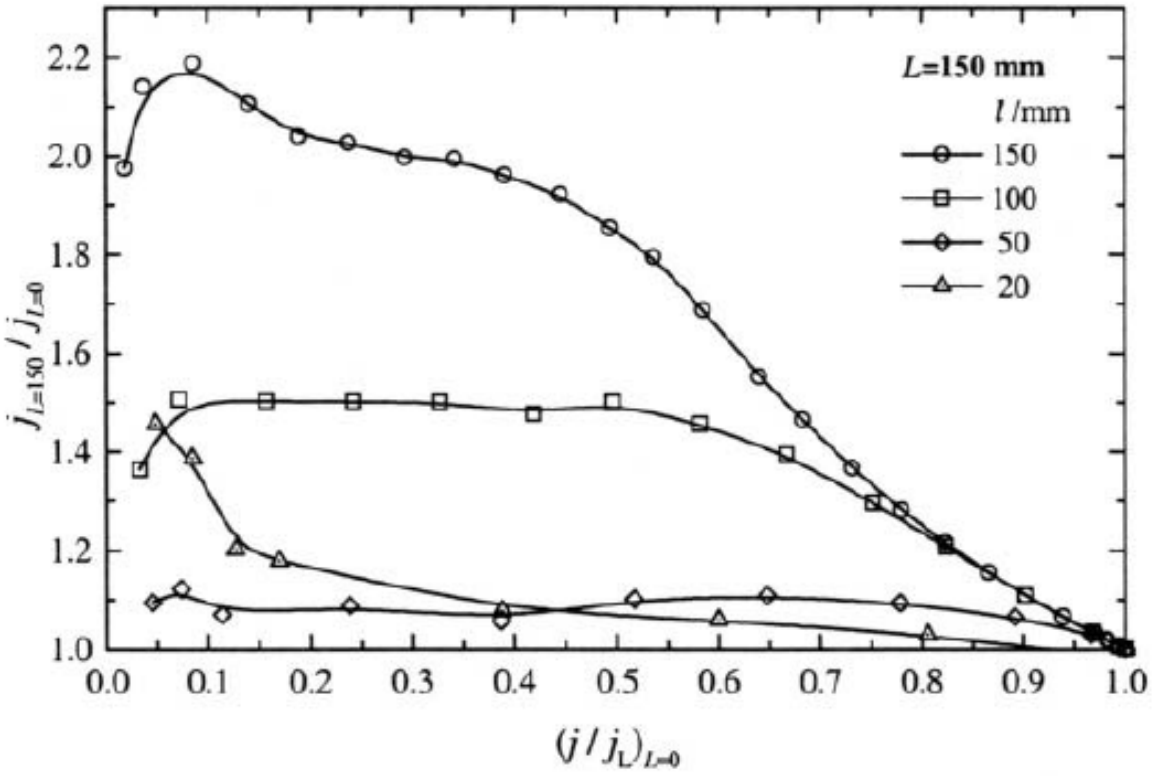

Figure 4.11. The $j_{L=150} / j_{L=0}$ ratio in the cell Cu|0.1 mol dm^{-3} $CuSO_4$, 0.1 mol dm^{-3} H_2SO_4|Cu with electrode edges–cell side wall distance L = 150 mm and different interelectrode distances a) l = 20 mm, b) l = 50 mm, c) l = 100 mm and d) l = 150 mm, as a function of the current density in a cell with L = 0, normalized relative the limiting diffusion current density. Data from Figs. 4.7-4.10.[13] (Reprinted with permission from the Serbian Chemical Society, Belgrade, Yugoslavia).

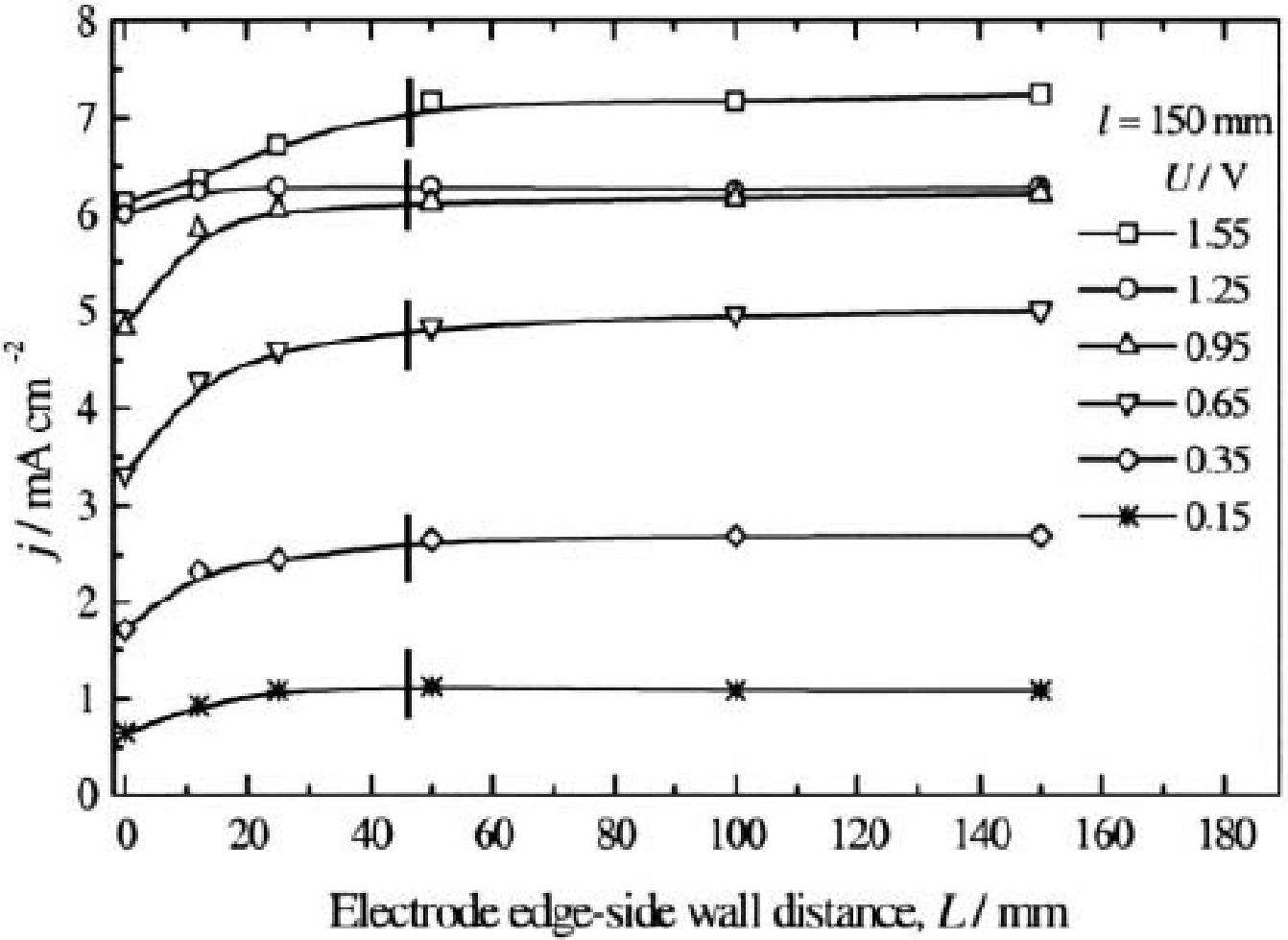

Figure 4.18. Current densities for different cell voltages as functions of the electrode edges – cell side wall distances in a cell with interelectrode distance l = 150 mm for the system Cu|0.1 mol dm^{-3} $CuSO_4$, 0.1 mol dm^{-3} H_2SO_4|Cu. Data from Fig. 4.10.[14] (Reprinted with permission from the Serbian Chemical Society, Belgrade, Yugoslavia).

Düşük Anod Potansiyelindeki Polarizasyon

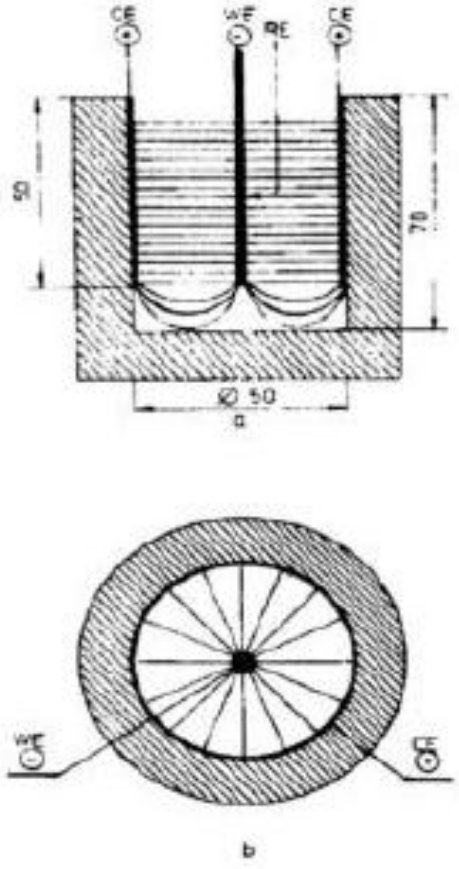

Figure 4.21. Current distribution in a cylindrical electrode geometry: a) front cross section, b) top cross section.[15] (Reprinted with permission of Elsevier Science).

$$U = E + \eta_a + \eta_c + RI \tag{4.37}$$

where R is the ohmic resistance of the electrolyte and I current in the cell, and for the tip of wire electrode:

$$U = E + \eta_{a,e} + \eta_{c,t} \tag{4.38}$$

where $\eta_{c,t}$ and $\eta_{a,e}$ are the overpotential at the tip of wire electrode and at the edge of the cylindrical anode, respectively, or after elimination of U-E from Eqs. 4.37 and 4.38

$$\eta_{a,e} + \eta_{c,t} = \eta_a + \eta_c + RI \tag{4.39}$$

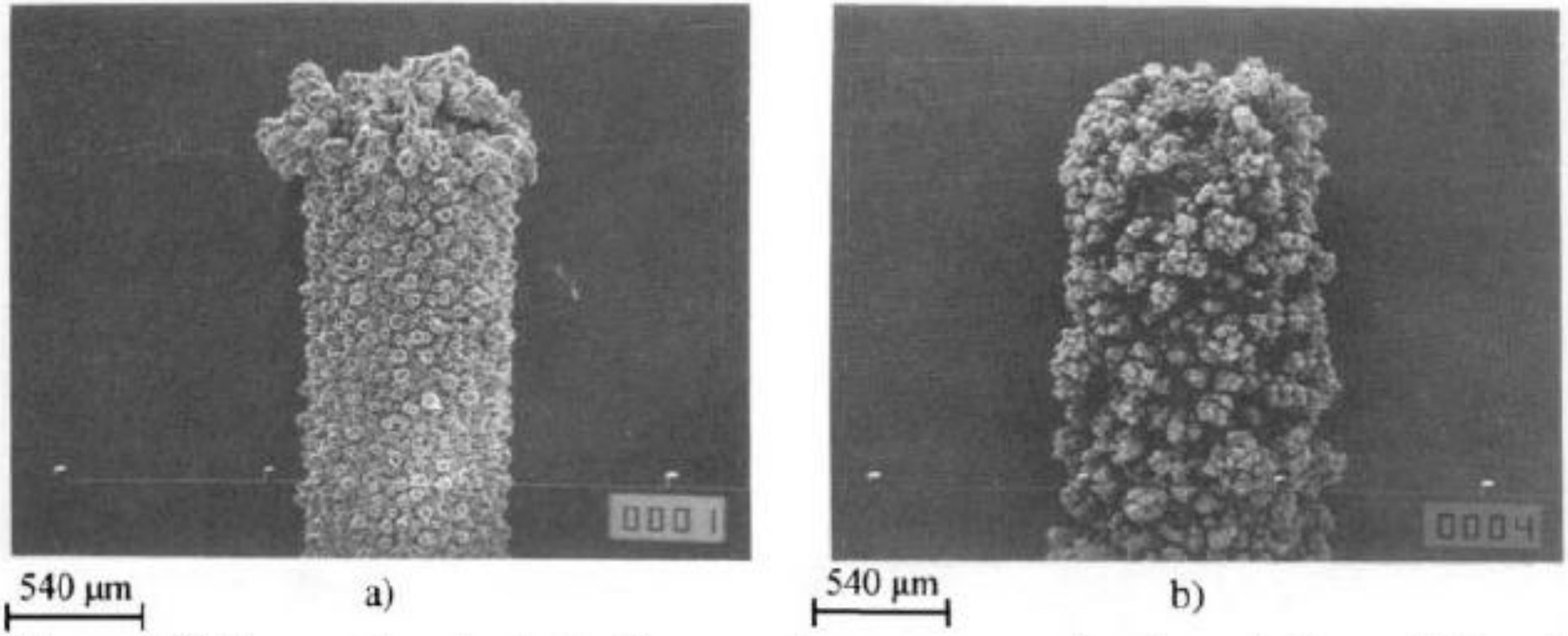

Figure 4.24. Copper deposit obtained on a stationary copper wire electrode from a) 0.1 mol dm^{-3} $CuSO_4$ b) 0.1 mol dm^{-3} $CuSO_4$ in 0.5 mol dm^{-3} H_2SO_4. Quantity of electricity 40 mA h cm^{-2}. Overpotential 250 mV.[15] (Reprinted with permission from Elsevier Science).

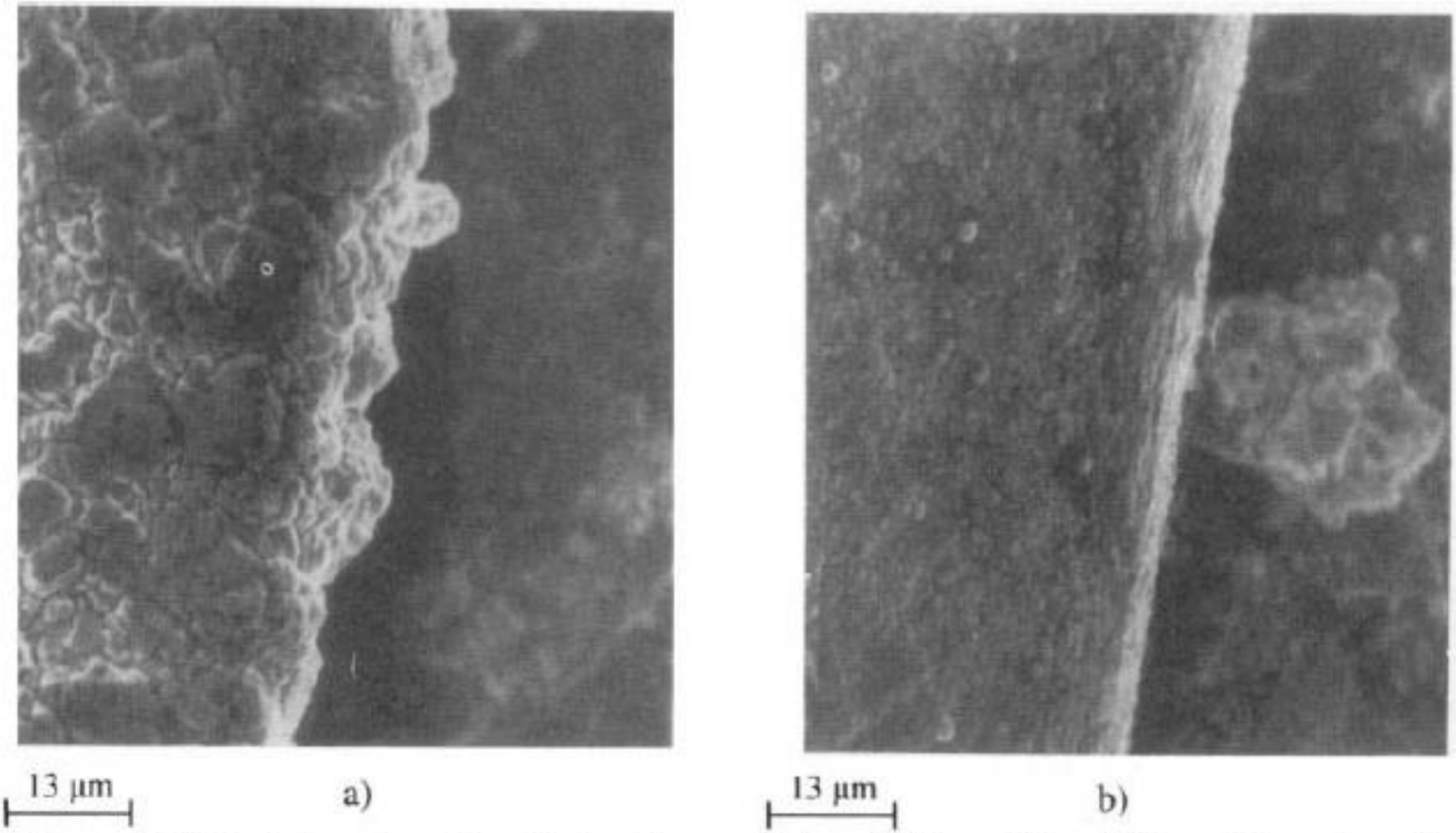

Figure 4.26. Cadmium deposits obtained from sulfate solution with additive, at the edge of a copper electrode. The thickness of deposit was 3µm. Deposition overpotential: a) 40 mV, b) 530 mV.[16] (Reprinted with permission from Elsevier Science).

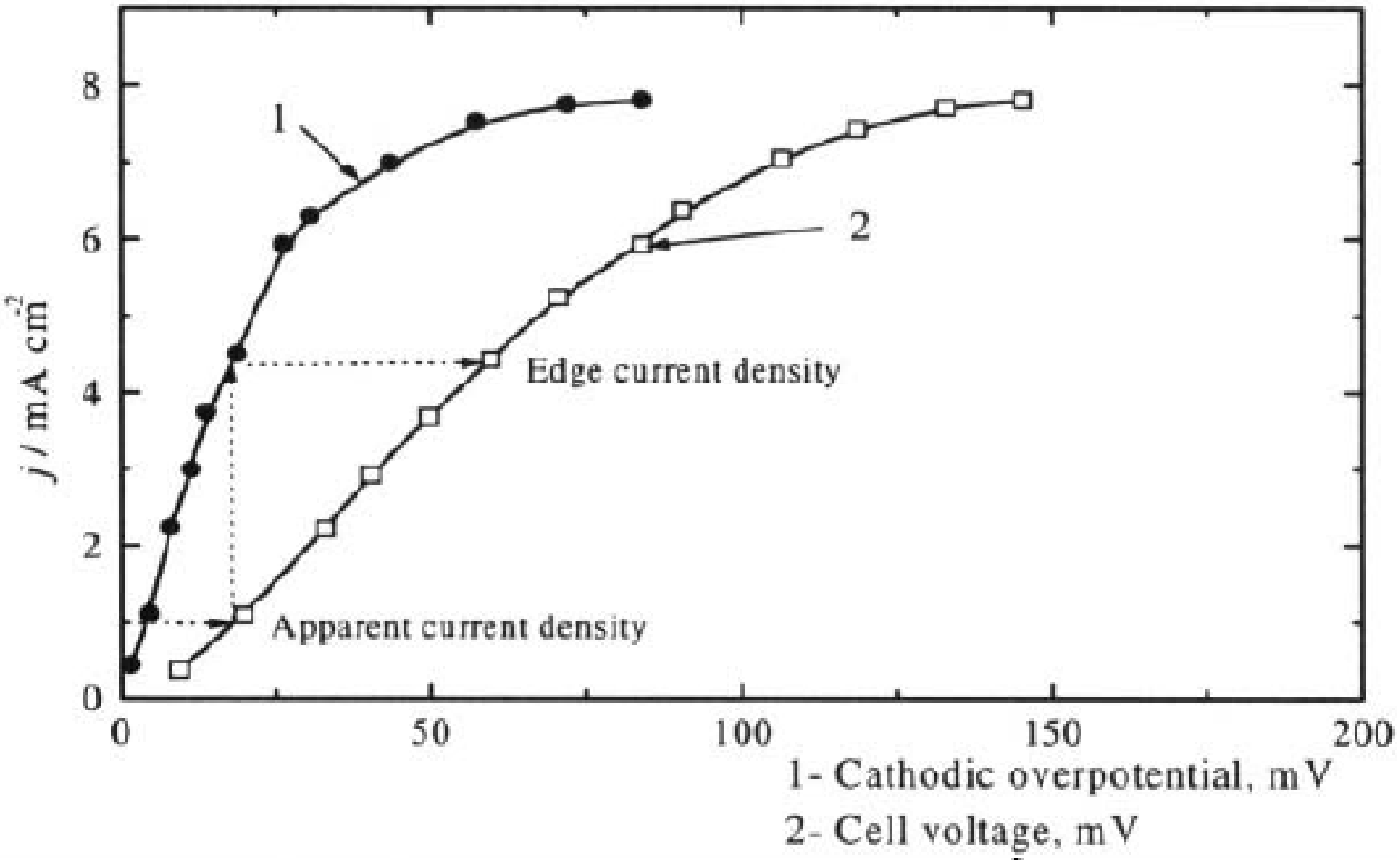

Figure 4.27. **Overpotential-apparent current density (1) and cell voltage-apparent current density (2) dependencies for deposition from the nitrate bath.[17] (Reprinted with permission from Elsevier Science).**

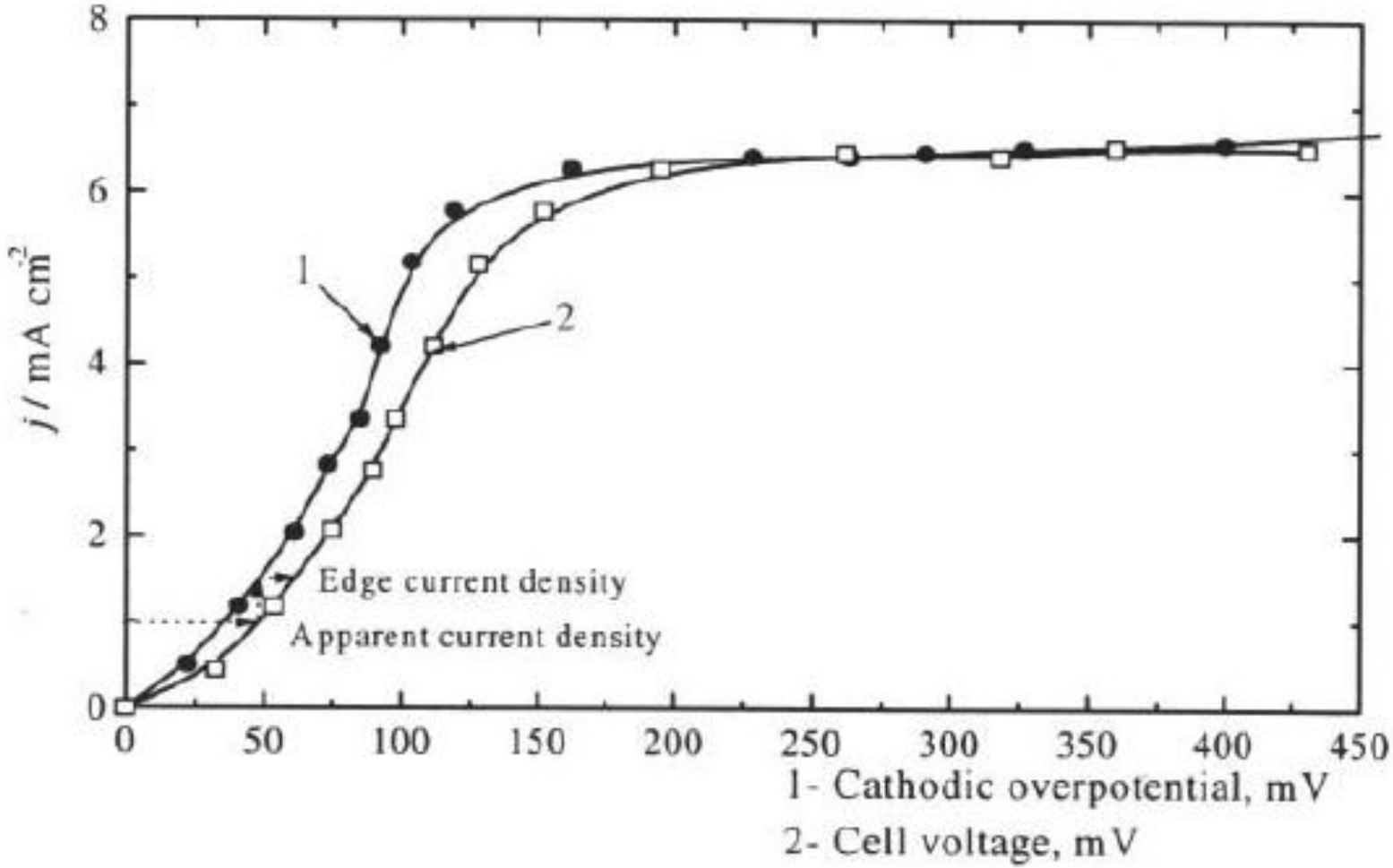

Figure 4.28. Overpotential-apparent current density (1) and cell voltage-apparent current density (2) dependencies for deposition from the ammonium complex bath.[17] (Reprinted with permission from Elsevier Science).

For the ammonium bath there is a region where deposition is under activation control because $j_0 < j < j_L$, $j_0 = 0.25$ **mA cm^{-2}** and a slope of **60 mV dec^{-1}**. Hence, nucleation occurs over all surface. For deposition from the ammonium bath, as predicted by Fig. 4.28, a more homogenous distribution of the deposit is obtained, which is illustrated in Figs. 4.29c and 29d.

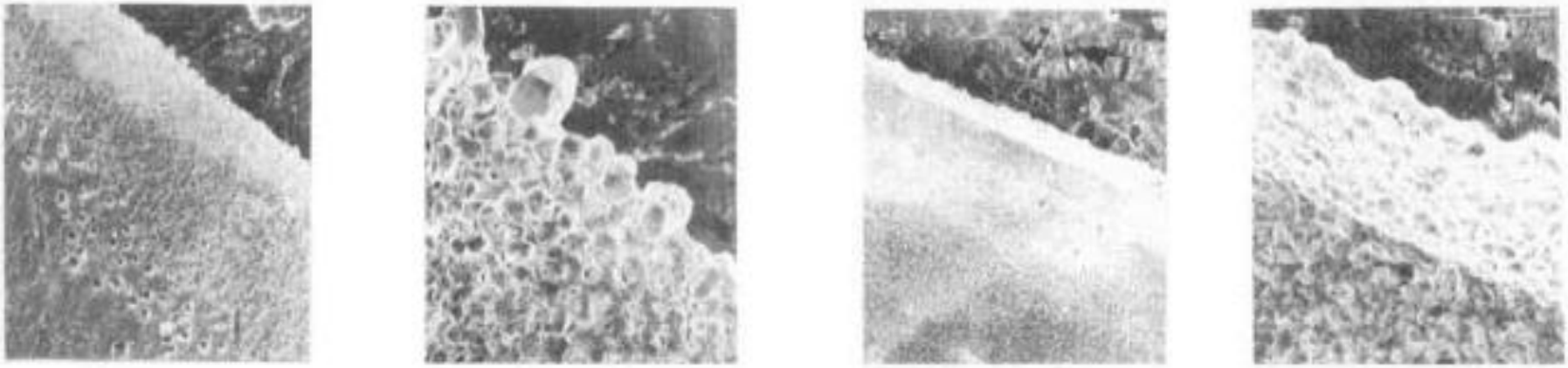

Figure 4.29. Silver deposits obtained at 1 mA cm^{-2} (deposition time, 40 min): a) nitrate bath; b) nitrate bath; c) ammonium complex bath; d) ammonium complex bath.[17] (Reprinted with permission from Elsevier Science).

Köse Etkisi

"Corner weakness" occurs in heavy deposits or electroforms at screened cathode parts *i.e.* corners. The deposit is thinner and at these areas,, in extreme cases, there is no deposition at all along the line of the corner bisector[18].

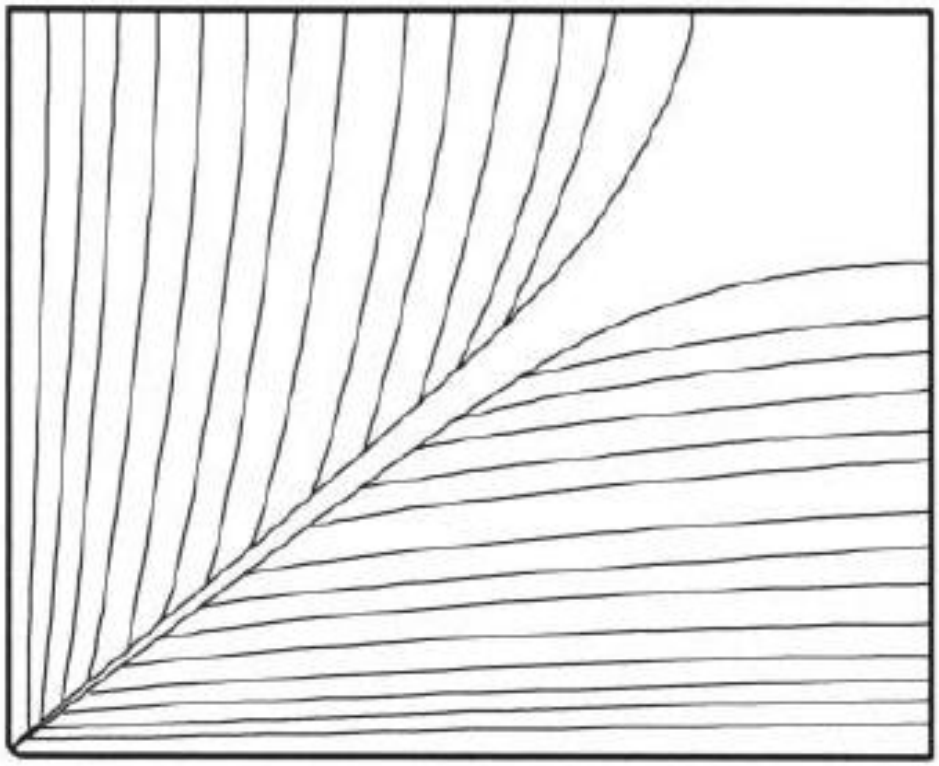

Figure 4.30. **Schematic representation of microphotographs illustrating the "corner weakness" effect. (From Popov and Stevanović[19] with the kind permission of the Serbian Chemical Society, Belgrade, Yugoslavia).**

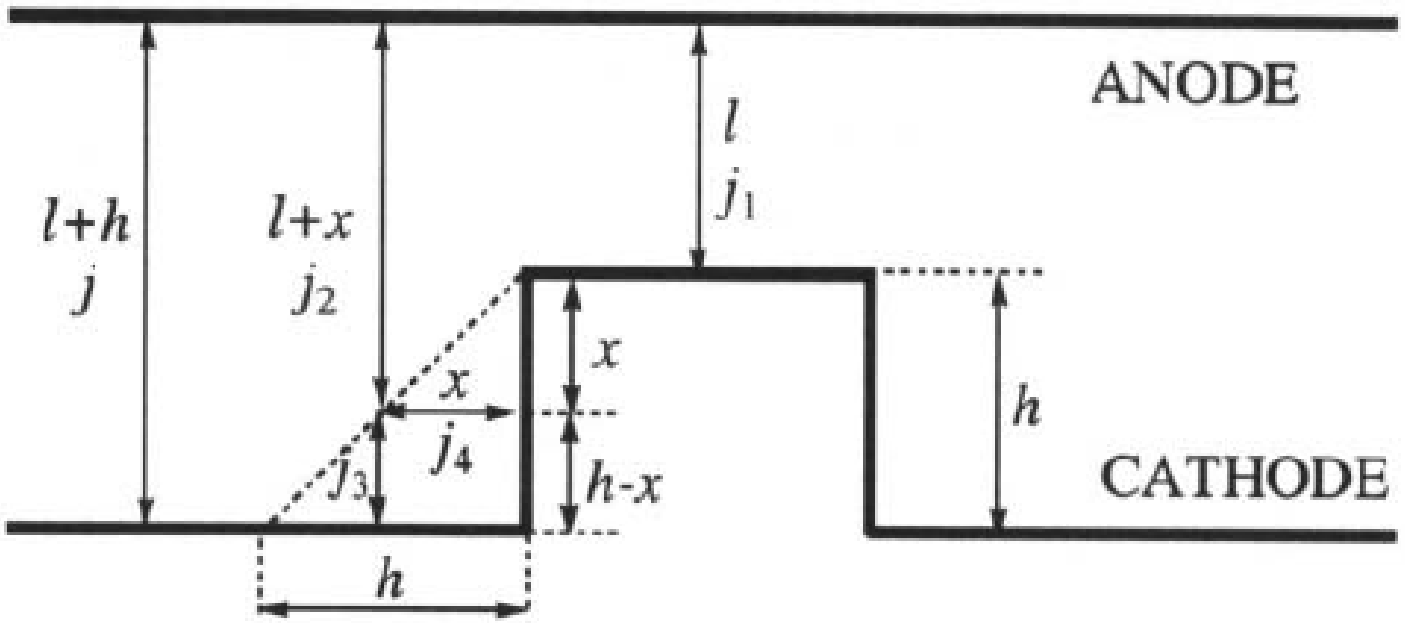

Figure 4.31. **Evaluation of a current distribution in the cell using the concept of current line division.[19] (Reprinted with permission from the Serbian Chemical Society, Belgrade, Yugoslavia).**

The ohmic potential drops along the current lines j and j_1 are given by Eqs. 4.47 and 4.48 respectively, asuming E=0.

$$U = \rho\,(l+h)j \tag{4.47}$$

$$U = \rho\, l j_1 \tag{4.48}$$

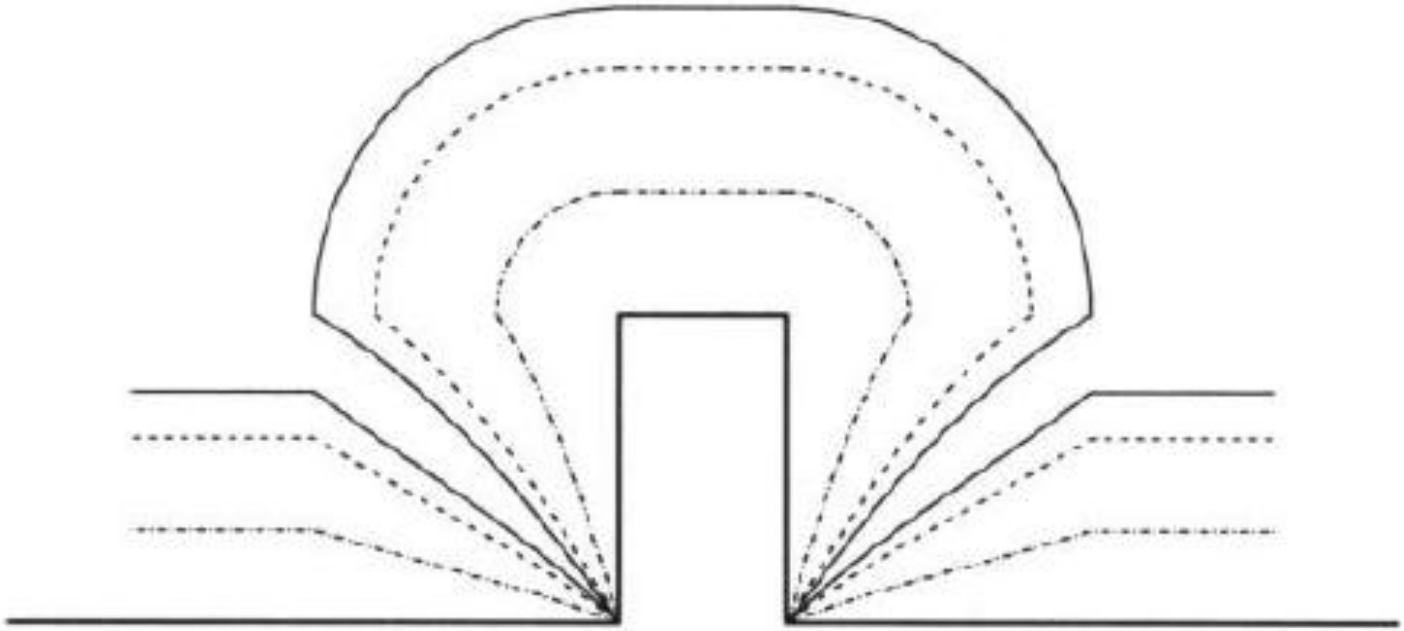

Figure 4.32. Simulation of a growth of the deposit from the model protrusion (h=5cm, l =15cm) calculated for pure ohmic control employing Eqs. 4.53 and 4.54.[19] (Reprinted with permission of the Serbian Chemical Society, Belgrade, Yugoslavia).

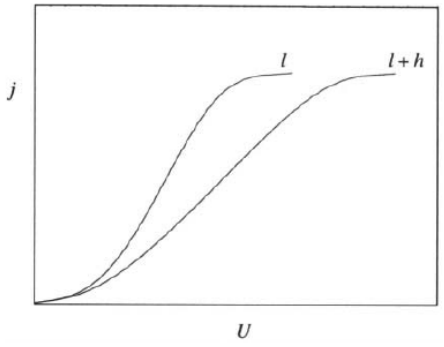

Figure 4.33. Cell voltage current curves for interelectrode distances l and $l + h$.[19] (Reprinted with permission from the Serbian Chemical Society, Belgrade, Yugoslavia).